Research Square

Preprints are preliminary reports that have not undergone peer review.
They should not be considered conclusive, used to inform clinical practice,
or referenced by the media as validated information.

The impact of injected peptide mass on small intestinal neuroendocrine tumor and normal organ somatostatin receptor expression; Measurements on 68Ga-DOTATOC-PET in a simulated therapy setting

Ezgi Ilan Rencber

ezgi.ilan@akademiska.se

Uppsala University Faculty of Medicine: Uppsala Universitet Medicinska fakulteten

Ulrika Jahn

Uppsala University Faculty of Medicine: Uppsala Universitet Medicinska fakulteten

Irina Velikyan

Uppsala University Faculty of Medicine: Uppsala Universitet Medicinska fakulteten

Mark Lubberink

Uppsala University Faculty of Medicine: Uppsala Universitet Medicinska fakulteten

Anders Sundin

Uppsala University Faculty of Medicine: Uppsala Universitet Medicinska fakulteten

Research Article

Keywords: Neuroendocrine tumors, Peptide Receptor Radionuclide Therapy, Peptide, Dosimetry, ”NET”, ”PRRT”, ”Si-NET”, ”68Ga-DOTATOC”, ”PET CT”, ”somatostatin receptors”

Posted Date: November 4th, 2026

DOI: https://doi.org/10.21203/rs.3.rs-11314658/v1

License: This work is licensed under a Creative Commons Attribution 4.0 International License.
Read Full License

The impact of injected peptide mass on small intestinal neuroendocrine tumor and normal organ somatostatin receptor expression; Measurements on ^{68}Ga-DOTATOC-PET in a simulated therapy setting

Ezgi Ilan Rencber[1, 2], Ulrika Jahn[1], Irina Velikyan[1,3], Mark Lubberink[1,2], Anders Sundin[1,3]

ezg.ilan@uu.se (EIR); ulrika.jahn@uu.se (UJ); irina.velikyan@kemi.uu.se (IV); mark.lubberink@uu.se (ML); anders.sundin@uu.se (AS).

[1] Molecular Imaging and Medical Physics, Department of Surgical Sciences, Uppsala University, Uppsala, Sweden,

[2.] Medical Physics, Uppsala University Hospital, Uppsala, Sweden,

[3.] Medical Imaging Centre, Uppsala University Hospital, Uppsala, Sweden

Correspondence: Ezgi Ilan Rencber ezgi.ilan@uu.se (EIR); Telephone: +4618 6112751. Department of Surgical Sciences, Radiology & Molecular Imaging, Uppsala University Hospital, SE-751 85 Uppsala, Sweden

Abstract

Background: The impact of systemic somatostatin analogs on tumor versus normal organ somatostatin receptors (SSR) in conjunction with peptide receptor radionuclide therapy (PRRT) has long been debated. In a previous ^{68}Ga-DOTATOC-PET/CT study, at 7 h post intravenous (iv) injection of a preload of 400 µg octreotide, the SSR expression in small intestinal neuroendocrine tumors was restored to baseline levels, but remained reduced by approximately 50% in liver, spleen and pancreas creating a "therapeutic window". The present study explored this "window" in a simulated PRRT setting in patients with disseminated Si-NETs, by firstly administer the 400 µg iv octreotide preload, and secondly 150 µg of iv octreotide at ^{68}Ga-DOTATOC-PET/CT, to identify possible organ protection and tumor response difference in all, large and small tumors.

Methods: Nine patients underwent three serial ^{68}Ga-DOTATOC-PET/CT examinations during two days, including both dynamic and static whole-body (WB) registrations. Each PET/CT session started with iv injection of 153 ± 30 MBq, 22.1 ± 6.7 µg (mean ± SD) ^{68}Ga-DOTATOC. Ten minutes before the last two PET/CT sessions, an extra iv infusion of 150 µg octreotide was administered, and five hours prior to the last PET/CT, an iv infusion of 400 µg octreotide was given. Measurements were performed of tumor uptake (mean SUV) and net influx rate (K_i), as well as SUV (mean) in abdominal organs blood and bone marrow (BM), utilized 50 % iso-contour volumes of interest.

Results: Over time, SUV and K_i in Si-NETs declined in parallel with rising peptide concentrations ($p < 0.05$) for the groups of all- and small tumors while the large tumor group showed no decline. A decline in SUV (30–50%) was observed in the abdominal organs at the second PET/CT scan (WB 2) ($p < 0.004$), performed in conjunction with 150 µg of iv octreotide, and the uptake in spleen and liver decreased further, at the third PET/CT scan (WB 3) ($p < 0.05$).

Conclusion: In the presence of peptide amounts similar to those administered at PRRT, Si-NET uptake might be reduced more in small than in large tumors cancelling the potential therapeutic benefits of a 400 μg iv octreotide preload.

Trial registration: Regional Ethics Comitté, Uppsala, Sweden, No. 2014/39. Registered 4 June 2018, https://etikprovningsmyndigheten.se/

Keywords: Neuroendocrine tumors, Peptide Receptor Radionuclide Therapy, Peptide, Dosimetry,”NET”, ”PRRT”, ”Si-NET”, ”68Ga-DOTATOC”, ”PET CT”, ”somatostatin receptors”

Declarations

Ethics approval and consent to participate

All procedures agreed with Good Clinical Practice guidelines as defined by the international Conference on Harmonization including international and Swedish regulations. All patients provided written informed consent. This study was approved by the Regional Ethics Committee, Uppsala, Sweden (No 2014/39).

Consent for publication

Not applicable

Availability of data and material

The datasets generated and/or analyzed during the current study are available from the corresponding author on reasonable request.

Competing interests

Non.

Funding

This work has not received external funding

Authors' contributions

Conceptualization A.S. and U.J., Methodology A.S., M.L. and E.I., Validation A.S., M.L., E.I., I.V. and U.J., Formal Analysis E.I., U.J. and A.S., Investigation E.I. and U.J., Data curation A.S., E.I. and U.J., Writing–Original Draft Preparation E.I., U.J. and A.S.; Writing–Review and Editing E.I., U.J. M.S., I.V. and A.S., Supervision A.S. All authors have read and agreed to the published version of the manuscript.

Acknowledgements

Our gratitude to Jonathan Sigfridsson for his outstanding help at the PET department.

List of abbreviations

SSA	somatostatin analog
SSR	somatostatin receptor
PRRT	peptide receptor radionuclide therapy
Si-NET	small intestinal neuroendocrine tumor
WB	whole body
BM	bone marrow
VOI	volume of interest
NETs	neuroendocrine tumors
DYN	dynamic
TACs	time-activity concentration curves
G1	grade 1
G2	grade 2
PET	positron emission tomography
CT	computed tomography
SUV	standard uptake value
K_i	net influx rate

Introduction

Neuroendocrine tumors (NETs) are rare, slow growing and heterogenous tumors that combine traits from the tissue of origin, with typical NET traits such as an overexpression of somatostatin receptors (SSR) in low grade tumors, and the capacity of hormone production [1]. NETs can be found in any tissue of the body and when derived from neuronal structures they can demonstrate a non-epithelial origin [2, 3]. They produce five different SSRs (1-5) originating from separate genes [4, 5] of which SSR2 dominates in most NETs [6, 7]. Only SSR5 is located intracellularly and is recruited to the cell surface at peptide stimulation, while SSR 1 to 4 are located and stored on the surface of the tumor cells [8, 9]. Somatostatin analogs (SSAs) generally bind to SSR2 and to a lesser extent on SSR3 and SSR5, but do not interact with SSR1 or SSR4 [10]. In several NET types, long-acting SSAs constitute the standard systemic treatment to decrease the patient´s hormonal symptoms [11] while short-acting SSAs are used for imaging with ^{68}Ga-DOTATOC, and peptide receptor radionuclide therapy (PRRT) with ^{177}Lu-DOTATATE. At stimulation, SSRs internalize instantly and recirculate within hours, with a delay of 2 h from stimulation, until new binding sites can be identified on the tumor cell surface [12, 13]. The complete receptor body restoration is considered to take about 16 to 24 h [14]. Tumor SSR2s were furter demonstrated to be rapidly internalised in a dose dependent fashion, when stimulated peri-operatively in humans [13]. The interaction between SSRs and SSAs has been a conundrum since the introduction of ^{68}Ga- and ^{177}Lu-labeled SSAs [15-19]. Hucovic et al. reported that continuous treatment with short acting SSAs affected the production of the five receptor subtypes differently [20], and long-term exposure to SSR agonists upregulates SSR2, more highly in tumors than in normal tissues, suggesting that a competitive binding from the supplemental treatment to the PRRT was negligible [14]. Despite these early findings, there has been a long standing recommendation to postpone SSA treatment before PRRT, to avoid possible competitive binding between unlabeled and labeled peptides [16]. Later, however, this

recommendation has been challenged by PET and PRRT studies, reporting unaffected ^{177}Lu-/^{68}Ga-DOTATATE uptake in tumors during continuous treatment with long-acting SSAs, [18, 19, 21, 22]. Similarly, a pre-dose of 50 µg short-acting octreotide before ^{68}Ga-DOTATOC injection, at PET/CT, produced lower normal organ uptakes, but with tumor uptake similar to that at baseline PET/CT performed without additional iv octreotide [23, 24]. In an earlier ^{68}Ga-DOTATOC-PET/CT study from our group, both large (≥4 mL) and small (>1–4 mL) Si-NET metastases showed full uptake (SUV) recovery within 4 hours after an iv bolus of 400 µg octreotide, as compared to the baseline ^{68}Ga-DOTATOC-PET, interpreted as full tumor SSR recovery, whereas in the normal abdominal organs (liver, pancreas and spleen) merely a fraction of the receptor body had recovered after 7 hours [25]. In that study, the peptide mass of the ^{68}Ga-DOTATOC preparation was the customary to the imaging situation (approximately 20 µg) and not adapted to that at PRRT (approximately 150 µg). The present study in Si-NET patients, therefore, was designed to determine if the earlier findings would remain in a PRRT simulated setting. We thus employed serial ^{68}Ga-DOTATOC-PET/CT to assess the dynamics of SSR invagination and recovery in all tumors, large respective small tumors and normal organs, and mimicking a PRRT through simultaneously administration of 150 µg octreotide before and after a 5-hour pre-load of 400 µg octreotide.

Method

PET Imaging

Nine PRRT native patients with disseminated Si-NET underwent three serial ^{68}Ga-DOTATOC-PET/CT (153 ± 30 MBq, 22.1 ± 6.7 µg mean ± SD) examinations during two consecutive days, according to the protocol shown in Figure 1. ^{68}Ga-DOTATOC was produced according to previously published routine procedures [25]. PET/CT utilized a digital time-of-flight PET/CT scanner (Discovery MI, GE Healthcare, Milwaukee Wisconsin, USA). All PET/CT scans

consisted of a 45-mimute dynamic investigation over the upper abdomen starting simultaneously with tracer injection, followed by a 1 h post injection whole-body scan according to clinical routine. The first PET/CT-scan was performed using the standard clinical peptide dose (20 µg). Five hours after the first PET/CT the patient received a ten-minute iv infusion of 150 µg octreotide (equivalent to the peptide amount at PRRT), immediately prior to the second ^{68}Ga-DOTATOC-injection and PET/CT examination. The second day, a preload iv injection of 400 µg octreotide was given in the morning and five hours later the third and last ^{68}Ga-DOTATOC PET/CT was performed, also preceded by an iv infusion of 150 µg octreotide. The dynamic scans reconstructed into 22-time frames as detailed previously [25] (Figure 1, Table 1).

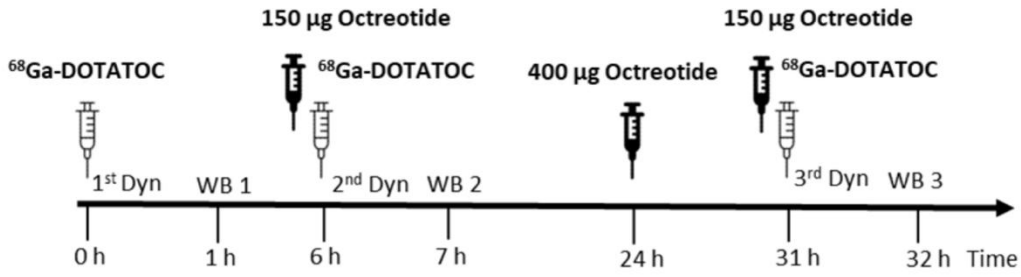


Figure 1. Flowchart of the ^{68}Ga-DOTATOC-PET/CT examination procedure during the two consecutive study days. Wherein WB and Dyn stand respectively for whole body acquisition and dynamic acquisition

Table 1. The ^{68}Ga-DOTATOC-PET/CT examination procedure during the two study days. pat: patient, iv: intravenous

	Day 1		**Day 2**	
Time	10 a.m.	3 p.m.	10 a.m.	3 p.m.
	Dynamic ^{68}Ga-DOTATOC-PET/CT of upper abdomen + Clinical WB PET/CT	150 µg Octreotide iv + Dynamic ^{68}Ga-DOTATOC-PET/CT of upper abdomen + WB PET/CT	400 µg Octreotide iv	150 µg Octreotide iv + Dynamical ^{68}Ga-DOTATOC-PET/CT of upper abdomen + WB PET/CT

Patients

Ten PRRT-naive patients with well differentiated low-grade (G1& G2) disseminated Si-NET, who were scheduled for a clinical ^{68}Ga-DOTATOC-PET/CT scan, provided their written

consent to participate in the study. Nine out of the ten patients were subject to treatment with long-acting SSAs and the one patient, without SSA treatment, discontinued the study due to abdominal pain after the first 150 µg octreotide injection while nine patients completed the study. Their median age was 63 years (range 40–78), and the time from Si-NET diagnosis to study start was median 2 (range 1–11) years (Table 2). There were 3 patients with low tumor burden (++) and solely small tumors, as rated by eyeballing on ^{68}Ga-DOTATOC-PET/CT, and 6 patients with high tumor burden (+++ and ++++). Four of these had both small and large tumors, one patient only small tumors, and one patient solely large tumors and all patients had liver metastases and five of them also had mesenteric metastases (Table 3).

Table 2. Patient characteristics. No: number, F: Female, M: Male, SSA: somatostatin analog

Patient no.	Age (years)	Sex	Time from diagnosis (years)	SSA medication
1	73	F	1	Somatuline 120 mg every 3rdweek
2	78	M	5	Sandostatin LAR 30 mg every 3rd week
3	54	M	7	Somatuline 120 mg every 4th week
4	40	M	2	Somatuline 120 mg every 3rd week
5	63	F	2	Sandostatin LAR 30 mg every 4th week
6	57	F	10	Sandostatin LAR 30 mg every 3rd week
7	69	F	2	Somatuline 120 mg every 3rd week
8	54	M	11	Sandostatin LAR 30 mg every 3rd week
9	75	F	2	Somatuline 120 mg every 3rd week

Tumors

The Si-NET metastases with the highest uptake were selected for analysis (n= 31), and the median value of each patient's included tumors was used for calculation of SUV (mean) and K_i (Table 3). Each patient´s tumors were further sub-grouped into a small and large group based on their sizes as measured on PET by 50% iso-contour volumes of interest (VOI); Thus, we formed three tumor groups: one representing all thirty-one tumors by the median value of each patient´s included tumors, one group consisting of the median value of the included large

tumors (≥4 mL n=15) of each patient and the third group consisting of the median value of the included small (1-4 mL n=16) tumors of each patient.

Table 3. Tumor characteristics. No: number, ND: not done, *:one missing value (Dyn1 PET/CT), ++,+++,++++, pleas se methods paragraph patients.

Patient	No. of analyzed tumors	No. of small tumors (>1–4 mL)	No. of large tumors (≥4 mL)	Si-NET Grade	Ki-67 %	Tumor mass and main location of metastases
1	5	4	1	G2	4	+++ /Liver
2	2	2		G1	< 2	+++ /Liver, Mesentery
3	1	1		G1	< 2	+ + /Liver
4	3	2	1	G1	2	+++ / Liver, Mesentery
5	1	1		ND	ND	++ /Liver, Mesentery
6	1	1		G1	2 / 18	++ /Liver
7	7	0	7	G1	2	+++ /Liver, Mesentery
8*	7	2	5	G2	5	+++ /Liver
9	4	3	1	G2	5	++++/Liver, Mesentery

Image analysis

The PET measurements were performed as earlier described in detail [25]. In all three whole-body PET-examinations (WB 1, 2 and 3), a 50% iso-contour (VOI) was defined using HERMIA Hybrid Viewer (version 7.0.2, Hermes Medical Solutions, Stockholm) to measure tumor SUV_{mean}. The SUV (mean) was also assessed in the normal abdominal organs - kidneys, spleen, liver, pancreas, together with bone marrow (lumbar vertebra), by using spherical VOI of 1.5 cm in diameter placed over representative parts of the organs. The organ VOIs was transferred and placed in the same position on all three whole-body PET examinations. SUV (mean) of blood was measured in the left atrium to minimize any influence from the myocardium.

Kinetic analysis of tumor data was performed on the dynamic PET-images (DYN 1, 2 and 3). Iso-contour VOIs, representing 50% of the maximum activity, were drawn on a summation image covering 20 to 45 minutes post-injection (frames 18–22) using HERMIA Hybrid Viewer.

These VOIs were then applied across all time frames of the dynamic series to generate tumor time–activity concentration curves (TACs). To obtain the input function, a spherical VOI with a diameter of 1 cm was placed over the descending thoracic aorta on a 0- to 180- second summation image (frames 1–10), where the bolus first-pass was clearly visible. This VOI was then projected onto all time frames to generate an arterial time–activity concentration curve. The image-derived input functions were calculated as previously described by multiplying the arterial time–activity concentration curve by a fixed plasma-to-whole-blood ratio of 1.6. The net influx rate (K_i) was determined using the Patlak graphical analysis method [26] [27].

Statistical methods

The median tumor SUV (the median value of the measured tumors in each patient) was calculated and compared across whole-body scans (WB 1, 2 and 3) using the Wilcoxon matched pairs signed rank test, with a significance level set at $p < 0.05$ (Prism, version 10.4,1; GraphPad Software, Inc.). The same Wilcoxon matched-pairs signed rank test comparison was conducted for testing of tumor-to-organ ratios. Furthermore, the organ SUV was compared between WB 1, WB 2, and WB 3 using the Wilcoxon matched pairs signed rank test, applying the same significance threshold. We also calculated the SUV ratios between the tumor groups and organs at each performed PET/CT scan.

Similarly, the median tumor K_i for each patient was determined in the dynamic acquisitions, and the relation between the three dynamic (DYN 1, 2 and 3) acquisitions was evaluated using a Wilcoxon matched pairs signed rank test (significance level set to $p < 0.05$). The relation between K_i and SUV was evaluated using linear regression and Pearson correlation.

Results

Tumors

Each incremental increase in administered peptide mass, resulted in a stepwise reduction of median SUV and K_i of respective patient's median values of all measured tumors, from the first iv injection of 150 µg octreotide (WB 2) to the 5-hour pre-load of 400 µg of octreotide before the last ^{68}Ga-DOTATOC-PET/CT in conjunction with 150 µg octreotide (WB 3), ($p < 0.05$) (Figure 2). However, when each patient's tumors were subdivided into a large ($\geq$4 mL) and a small (1–4 mL) group, the large tumor group merely showed a tendency of reduction in SUV from WB 1 to WB 3 thus strictly not significant ($p = 0.062$), while the group of small tumors reduced the uptake significantly at each step ($p < 0.05$) (Figure 3).

The development of respective measured tumors of each patient is charted together with each patient's tumor burden through eyeballing (Supplemental Figure 1).

Normal organs

At WB 2, performed in conjunction with the first iv injection of 150 µg octreotide, SUV in all measured abdominal organs decreased as compared to the baseline WB 1 ($p < 0.004$) (Figure 4). At PET/CT five hours following an iv 400 µg preload of octreotide (WB 3), also performed in conjunction with an iv injection of 150 µg octreotide, a further decrease in SUV was seen in the liver and spleen ($p < 0.05$) (Figure 4). From the baseline PET/CT until WB 3 the total uptake reduction was 50% in the spleen, 45% in the liver and 30% in the pancreas while the SUV in the kidneys was reduced only at WB 2 (20% of baseline WB 1) remained unchanged at WB 3 (Supplemental Figure 2). In contrast to the measured abdominal organs, bone marrow (vertebral body) increased between WB 1 and WB 2 but remained at a similar level in WB 3. A similar temporal SUV pattern was found in blood (measured in the left atrium) that increased in all

patients (n = 9) between WB 1 and WB 2 but was unchanged at WB 3 (Figure 4). In this study, the correlation between SUV and K_i became linear when the peptide concentrations were high at the second and third ^{68}Ga-DOTATOC-PET/CT imitating PRRT (R^2 = 0.87 and 0.90 respectively) (Figure 5).

The development of respective measured organ of each patient is charted together with each patient's tumor burden through eyeballing (Supplemental Figure 3).

The tumor-to-kidney and tumor-to-pancreas ratios were similar at WB 1 and WB 2, but dropped significantly at WB 3, after the 400 µg preload of iv octreotide 5-hour, in contrast to both the tumor-to-spleen and tumor-to-liver ratios, which increased between WB 1 and WB 2, but remained unchanged at WB 3, (Supplemental Figure 4).

Discussion

This study assessed the effect of a 400µg iv preload of octreotide on the uptake (SUV) in Si-NET metastases versus that in normal organs and tissues, measured by ^{68}Ga-DOTATOC-PET/CT in conjunction with an additional iv injection of 150µg octreotide to simulate a PRRT setting. In a previous clinical study, a potential "therapeutic window" for PRRT was created by the rapid full recovery of the tumor SSRs expression, but still to approximately 50% blocked SSRs in most normal tissues, 7 h after a 400 µg iv preload of octreotide as measured by conventional ^{68}Ga-DOTATOC-PET/CT. The current clinical study was therefore conducted by means of serial ^{68}Ga-DOTATOC-PET/CT, in a simulated PRRT setting. (Figure 1).

Only tumors larger than 1 mL, (spherical 50% cut-off VOIs on PET), were considered for measurements to attain reasonable accuracy in the quantification, owing to the problems with

partial volume effects and reduced test-retest reproducibility in the measurements of smaller lesions. The 9 included Si-NET patients had in total 31 measured tumor lesions, and to assess any differences related to tumor size these tumors were further divided into a group of 15 large tumors (≥4 mL) and another group of 16 small lesions (1–4 mL) and charted for each patient, together with an assessment of the patients´ tumor burden estimated through eyeballing on baseline ^{68}Ga-DOTATOC-PET/CT and expressed according to an arbitrary scale (+ to +++) (Supplemental Figure 1). For statistically accurate representation of each patient's measured tumors considering the various numbers of tumors between patients, the calculations of SUV and K_i were based on the median values of all measured tumors per patient.

At 5h following the 400 µg iv octreotide preload, we were not able to reproduce the previously created "therapeutic window", when in the current experimental setting peptide amounts corresponding to that at PRRT (150 µg) were injected in conjunction with ^{68}Ga-DOTATOC-PET/CT (DYN 3 and WB 3). The tumor SUV in the group of all tumors decreased incrementally between the three PET/CT scans ($p < 0.05$). However, in the further analysis between the two different tumor sizes, large (≥4 mL) and small (>1–4 mL), the latter group demonstrated a similar pattern as for the group of all tumors ($p < 0.05$), while the large tumors merely showed a tendency of decline in SUV from WB 1 to WB 3, which however did not reach statistical significance ($p = 0.062$) (Figure 2). Hence, the 150 µg of iv octreotide in the present study was enough to bind to and internalize a sufficient number of Si-NET SSRs in the group of all and small tumors, thus, eliminating the potentially favorable "therapeutic window" of the iv octreotide preload, in contrast to the group of large tumors. Some benefit by the preload of 400 µg iv octreotide was found for the spleen and liver, the SUVs of which still were reduced, but not for tumors, kidneys, pancreas or bone marrow (Supplemental Figure 2).

The present results partly differ from an earlier retrospective study (2006-2009), in a mixed population of Si-NET and pancreatic NET (P-NET) patients, that established no influence on the tumor SSR expression at the first PRRT cycle, as measured on 24-hour SPECT, when given either a high or low amount of peptide in the ^{177}Lu-DOTATATE preparation [28]. In that study, an early method for tumor dosimetry was used, originally developed for dosimetry measurements of the kidneys. At the time, those results corresponded to what Sabet et al. report on P-NET measurements of SUV (max) immediately before and after a PRRT session, using two different amounts of iv octreotide (180 µg and 300 µg) administered in conjunction with PRRT and measured by ^{68}Ga-DOTATOC-PET/CT [21].

Although, the group of large tumors in our present study responded with a nonsignificant decline at the third PRRT simulated ^{68}Ga-DOTATOC-PET/CT, equal to the findings of Jahn et al. and Sabet et al., the groups of all and small tumors in the present study responded differently by reducing their uptake. As for the response of the organs our present findings were similar to those described by Sabet [21].

Regarding the difference in findings between parts of our present results and the two earlier studies, the continuous SSR saturating effect by iv octreotide in two of the tumor groups in the present study, might possibly be due to size differences but possibly also due to further development of the precision in the applied dosimetry method, and the difference in reported tumor types. Thus, while the study of Sabet et al. focused on patients with P-NETs, and our earlier study was a mixture of Si-and P-NETs, the present study exclusively held Si-NETs. One factor that might affect a difference in SUV uptake between P-NETs and Si-NETs is the relation between the tumor vessels and tumor cells and tumor nests in respective tumor type, as defined by Scoazec. In his work he described that mature tumor vessels and tumor cells in P-NETs are

in close admixture, as opposed to typical small intestinal NETs, where most vessels run within the stroma at a distance from tumor nests [29]. This difference in vascularization between NET-types may thus influence the tumor uptake of radiolabeled peptides in a dissimilar way. Our previously reported findings of differences between pancreatic NETs and Si-NETs [30] was the reason why only Si-NET patients were included in the previous and present studies on peptide blocking.

This study raises the question whether there might be a difference in the sensitivity to peptide stimulation between large and small Si-NETs. One tampering factor is that the selection of large tumor in this study to a large extent emanated from one person (7/15) and the number of patients with large tumors were no more than five, we believe it is urgent to explore this question further with larger numbers of tumors and patients due to the implication it might have on the design of PRRT.

The SUV in all measured normal abdominal organs decreased at WB 2 (performed with 150 µg additional peptide) (Figure 3), similar to the results in numerous previous reports [19, 21-24, 31]. The SUV measurements of the kidneys represent a combination of endogenous uptake by SSR 2 expressing cells in vasa recta [32], and in the glomeruli, the tubular cells of the cortex and the ascending limb of Henle´s [33] but also the excretion of the blood activity, where approximately 20% of the administered radioactivity is excreted into the urine during the first two hours [34]. The kidney SUV was similar at WB 2 and WB 3, and thus unaffected by the 400 µg iv octreotide preload, and this was surprisingly also the case for the pancreas (Figure 3). The SUV in the spleen and liver however further decreased by the 5-hour preload of 400 µg iv octreotide (Figure 3), in line with our previous findings [25]. The SUV in blood was measured in the left atrium, to minimize the potential influence of the myocardium. The

incremental blood SUV increase in the serial PET/CT scans was expectedly similar to that in bone marrow, with its very low density of SSR2 expressing cells, as is earlier identified and reported [35].

The 400 µg iv octreotide preload was consequently unfavorable regarding the tumor-to-normal organ ratios in our experimental setup. The 150 µg of iv octreotide used in conjunction with PET/CT scanning to simulate the situation at PRRT further internalized the tumor SSRs thus reducing all ratios except for the tumor-to-spleen one (Supplemental Figure 4).

Production of a high specific radioactivity ^{177}Lu-DOTATATE/DOTATOC preparation may therefore be beneficial. With modern radiochemistry laboratory procedures, 7.4 GBq of ^{177}Lu may possibly be conjugated to 50 µg of peptide, or perhaps even less. This needs to be assessed in further experimental studies.

Our study has several limitations. We are aware that our results should be considered with caution due to the small patient group, and consequently a limited number of observations. Although we excluded tumors less than 1 mL, there are still inherent uncertainties related to quantifying the SUV in small tumors, thus necessitating further studies in larger groups of patients. The notion of a difference in vascularity between Si-NETs and P-NETs ought to be considered, as it might have an influence on the uptake of radiolabeled SSAs. This in combination with other differences between NET types, may therefore make comparisons with results from previous studies less valid, when performed in patient groups with a mixture of NET-types.

A strength of our study is the within-patient assessments of the effects of the subsequently administered iv octreotide, made possible by the serial PET/CT scanning using the same PET/CT scanner. Most patients (6/9) were not only represented by their largest measurable tumor but by the median value of two to seven tumors, probably being more representative of the patients´ tumor load. Further, the study was performed in a controlled experimental setting mimicking PRRT, but in contrast to the real PRRT situation, our experimental setting did not for ethical reasons employ iv amino acids for kidney protection, introducing a potential bias in the PET measurements, although the situation in this regard was similar for both tumors and the various normal organs.

Conclusion

In the presence of peptide amounts similar to those administered at PRRT, Si-NET uptake might be reduced more in small than in large tumors cancelling the potential therapeutic benefits of a 400 µg iv octreotide preload.

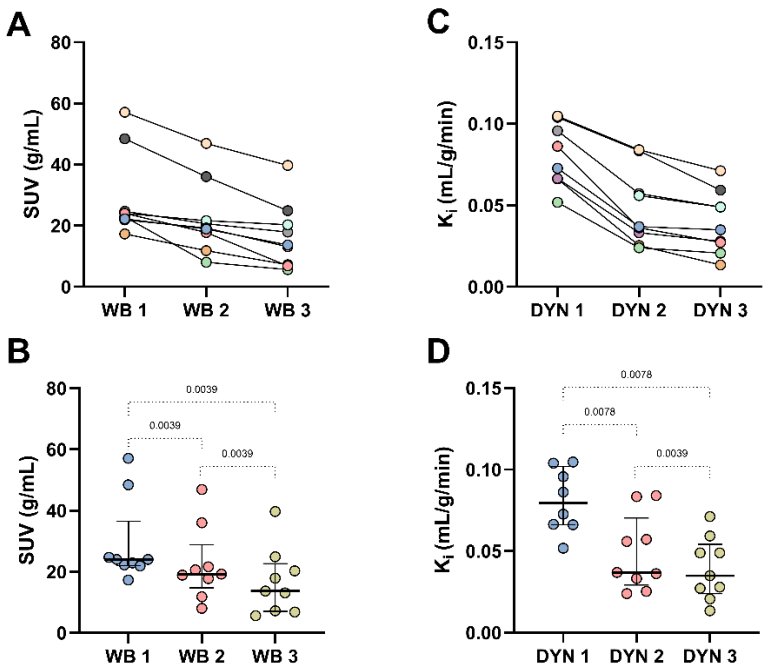


Figure 2. Median tumor value of SUV (mean) and median tumor value of K_i for each patient (A and B), Figures B and D show scatter dot plots, and the solid line represents median and interquartile range. SUV: standard uptake value, DYN; Dynamic PET WB: whole body PET.

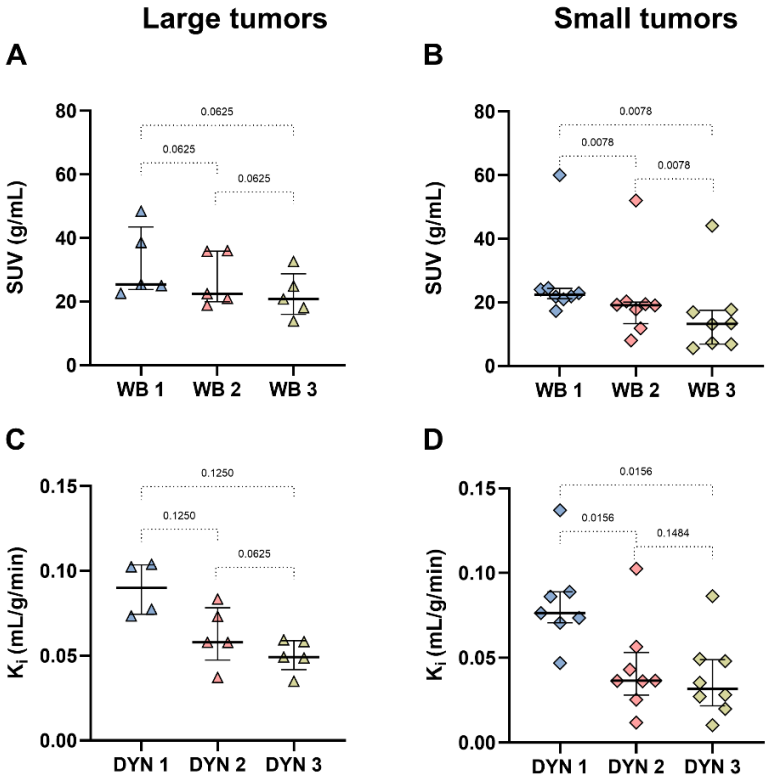


Figure 3. SUV (mean) in large and small SI-NETs. A and C represent the median value of respective patient's large tumors while B and D represent respective patient's small tumors. SUV: standard uptake value, WB: whole body PET.

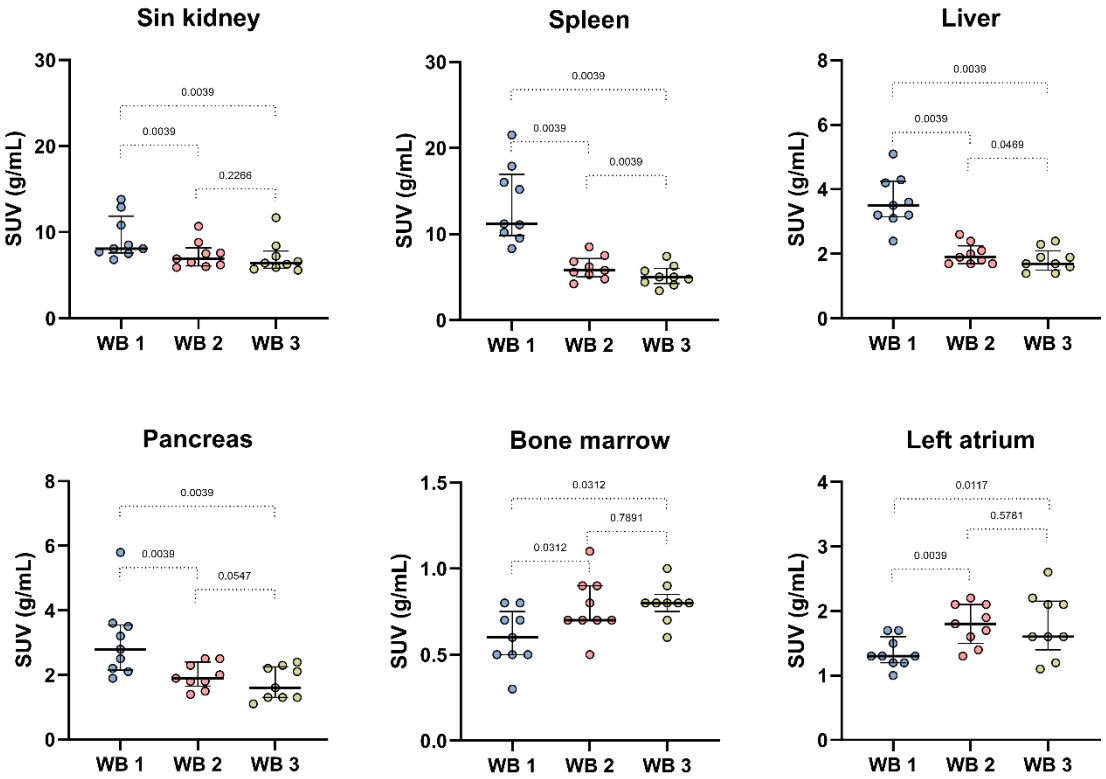


Figure 4. Scatter dot plots of SUV (mean) in the large abdominal organs, bone marrow and whole blood in left atrium for all patients (n=9). As the results were similar in both kidneys only the left (sin) kidney is presented. The solid lines represent the median, and the interquartile range. SUV: standard uptake value, WB: whole body PET.

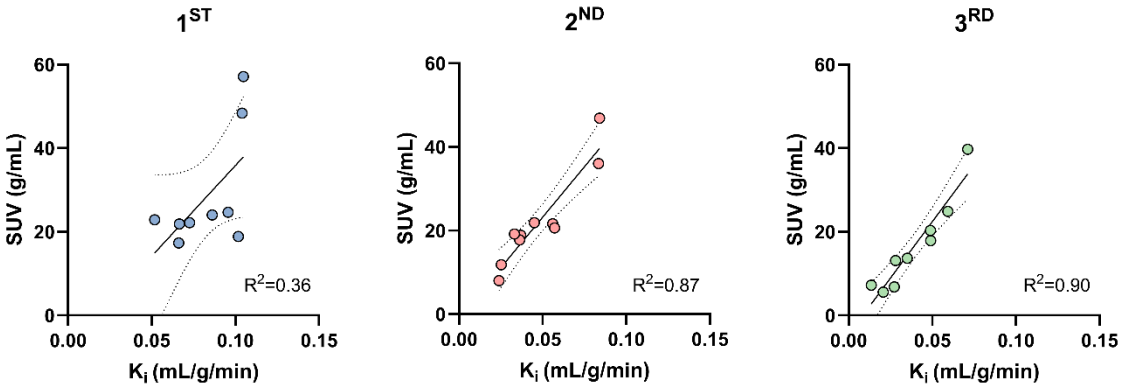
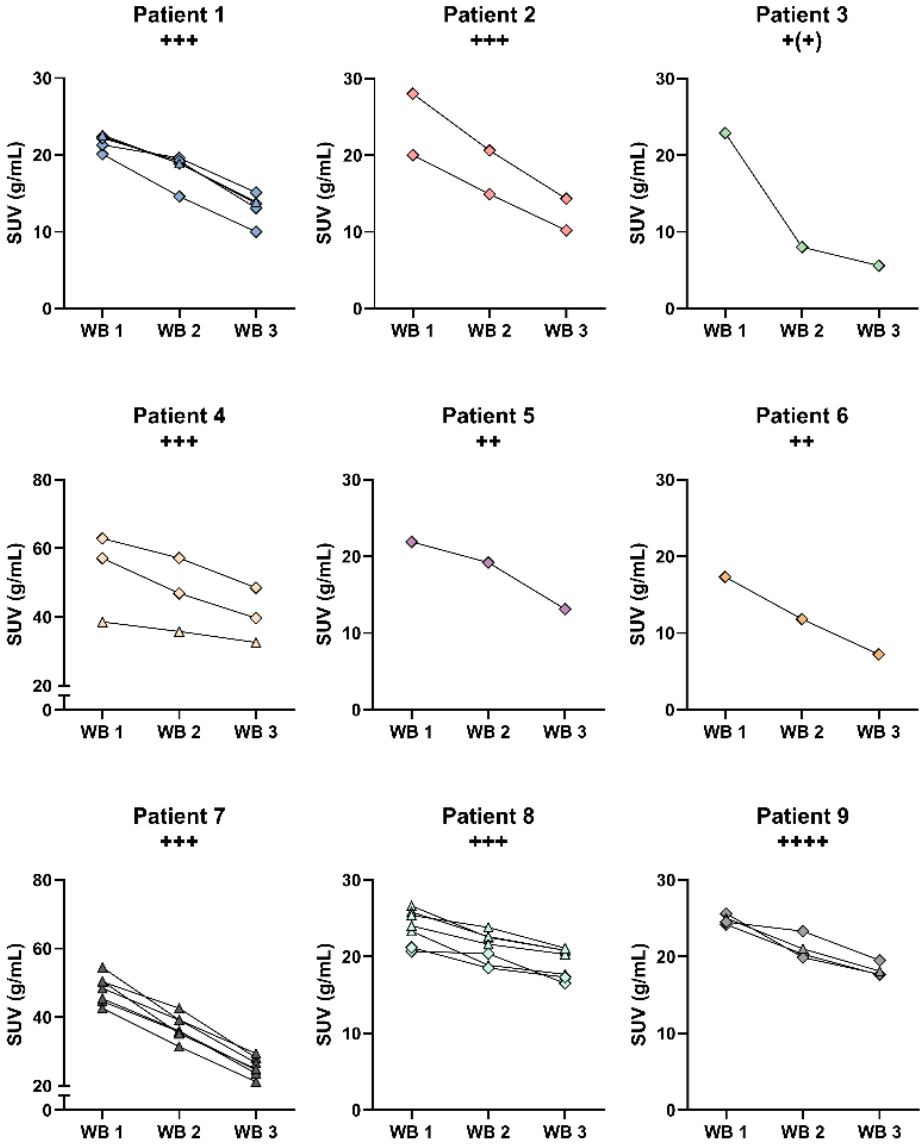
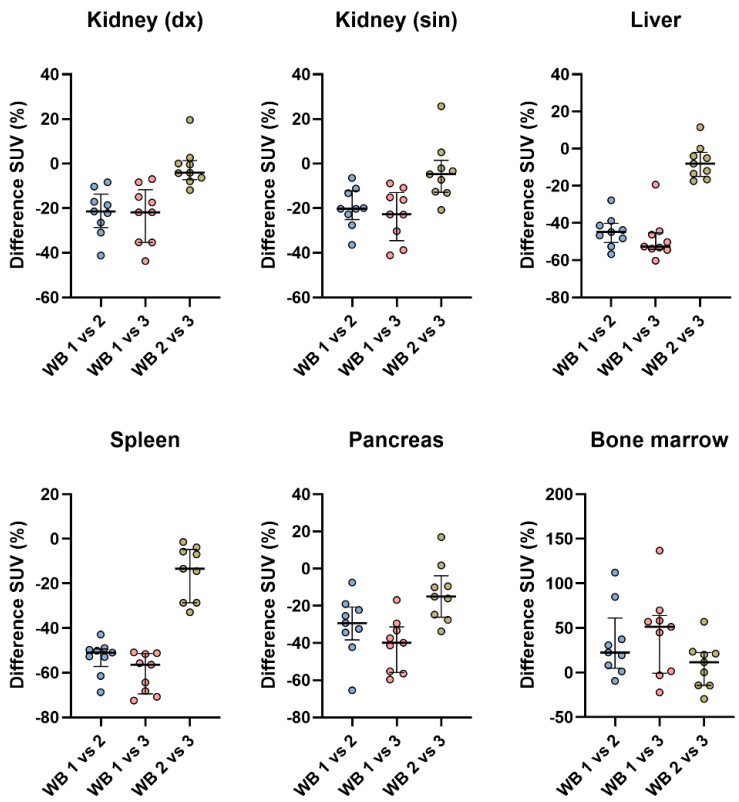


Figure 5. Correlation between SUV and K_i of the median values of each patient's tumors at the first, second and third PET/CT. SUV: standard uptake value, K_i: tumor net influx rate.

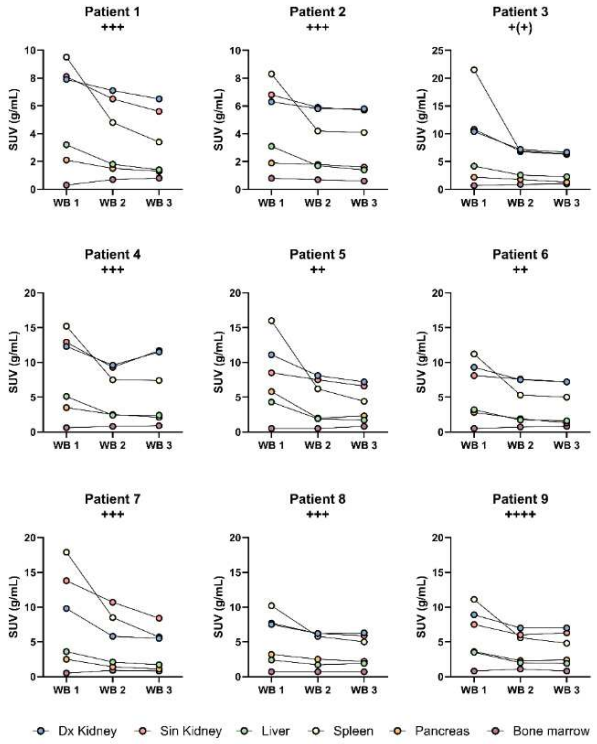
Supplemental Figures



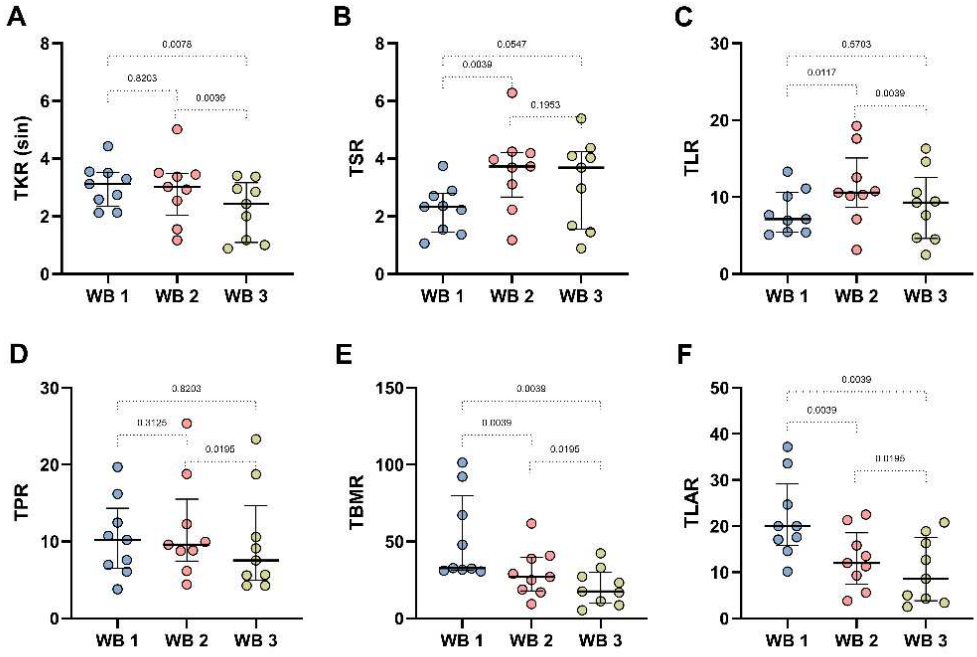
Supplemental Figure 1. SUV (mean) for respective tumor/-s of each patient. The number of "+" indicate the patient´s tumor burden. Data shown for large (Δ) respectively small (◊) tumors, and each color represents one patient. SUV: standard uptake value, WB: whole body PET.



Supplemental Figure 2. Percentage-based differences in SUV (mean) between WB 1 to WB 3 for organs. WB, whole body PET.



Supplemental Figure 3. SUV (mean) in the abdominal organs and bone marrow of each patient with increasing peptide content. The colors identify each organ as indicated. Plus-marks indicate tumor burden from eye-baling. SUV: standard uptake value, WB: whole body PET.



Supplemental Figure 4. Tumor to kidney ratio (TKR) in left kidney, the right kidney showed identical uptake (not shown), and tumor to spleen ratio (TSR) and tumor to bone marrow ratio (TBMR) and tumor to blood ratio (left atrium) (TLAR) at WB 1, 2 and 3. For calculation, the SUV (mean) of each patient's median tumor out of all measured tumors; In the figures, the solid line represents median and interquartile range. SUV: standard uptake value, BM: bone marrow, WB: whole body PET.

References

1. Schonbrunn A, Tashjian H, Jr. Characterization of functional receptors for somatostatin in rat pituitary cells in culture. J Biol Chem. 1978;253:6473-83.
2. Rindi G, Klimstra DS, Abedi-Ardekani B, Asa SL, Bosman FT, Brambilla E, et al. A common classification framework for neuroendocrine neoplasms: an International Agency for Research on Cancer (IARC) and World Health Organization (WHO) expert consensus proposal. Mod Pathol. 2018;31:1770-86. doi:10.1038/s41379-018-0110-y.
3. Rindi G, Mete O, Uccella S, Basturk O, La Rosa S, Brosens LAA, et al. Overview of the 2022 WHO Classification of Neuroendocrine Neoplasms. Endocr Pathol. 2022;33:115-54. doi:10.1007/s12022-022-09708-2.
4. Yamada Y, Post SR, Wang K, Tager HS, Bell GI, Seino S. Cloning and functional characterization of a family of human and mouse somatostatin receptors expressed in brain, gastrointestinal tract, and kidney. Proc Natl Acad Sci U S A. 1992;89:251-5. doi:10.1073/pnas.89.1.251.
5. Kluxen FW, Bruns C, Lubbert H. Expression cloning of a rat brain somatostatin receptor cDNA. Proc Natl Acad Sci U S A. 1992;89:4618-22. doi:10.1073/pnas.89.10.4618.
6. Wild D, Macke HR, Waser B, Reubi JC, Ginj M, Rasch H, et al. 68Ga-DOTANOC: a first compound for PET imaging with high affinity for somatostatin receptor subtypes 2 and 5. Eur J Nucl Med Mol Imaging. 2005;32:724. doi:10.1007/s00259-004-1697-4.
7. Sharif N, Gendron L, Wowchuk J, Sarret P, Mazella J, Beaudet A, et al. Coexpression of somatostatin receptor subtype 5 affects internalization and trafficking of somatostatin receptor subtype 2. Endocrinology. 2007;148:2095-105. doi:10.1210/en.2006-1266.
8. Stroh T, Jackson AC, Sarret P, Dal Farra C, Vincent JP, Kreienkamp HJ, et al. Intracellular dynamics of sst5 receptors in transfected COS-7 cells: maintenance of cell surface receptors during ligand-induced endocytosis. Endocrinology. 2000;141:354-65. doi:10.1210/endo.141.1.7259.
9. de Herder WW, Hofland LJ, van der Lely AJ, Lamberts SW. Somatostatin receptors in gastroentero-pancreatic neuroendocrine tumours. Endocr Relat Cancer. 2003;10:451-8. doi:10.1677/erc.0.0100451.
10. Breeman WA, Kwekkeboom DJ, Kooij PP, Bakker WH, Hofland LJ, Visser TJ, et al. Effect of dose and specific activity on tissue distribution of indium-111-pentetreotide in rats. J Nucl Med. 1995;36:623-7.
11. Bauer W, Briner U, Doepfner W, Haller R, Huguenin R, Marbach P, et al. SMS 201-995: a very potent and selective octapeptide analogue of somatostatin with prolonged action. Life Sci. 1982;31:1133-40. doi:10.1016/0024-3205(82)90087-x.
12. Waser B, Tamma ML, Cescato R, Maecke HR, Reubi JC. Highly efficient in vivo agonist-induced internalization of sst2 receptors in somatostatin target tissues. J Nucl Med. 2009;50:936-41. doi:10.2967/jnumed.108.061457.
13. Reubi JC, Waser B, Cescato R, Gloor B, Stettler C, Christ E. Internalized somatostatin receptor subtype 2 in neuroendocrine tumors of octreotide-treated patients. J Clin Endocrinol Metab. 2010;95:2343-50. doi:10.1210/jc.2009-2487.
14. Froidevaux S, Hintermann E, Torok M, Macke HR, Beglinger C, Eberle AN. Differential regulation of somatostatin receptor type 2 (sst 2) expression in AR4-2J tumor cells implanted into mice during octreotide treatment. Cancer Res. 1999;59:3652-7.

15. Bakker WH, Krenning EP, Reubi JC, Breeman WA, Setyono-Han B, de Jong M, et al. In vivo application of [111In-DTPA-D-Phe1]-octreotide for detection of somatostatin receptor-positive tumors in rats. Life Sci. 1991;49:1593-601. doi:10.1016/0024-3205(91)90053-e.
16. Kwekkeboom DJ, Krenning EP, Lebtahi R, Komminoth P, Kos-Kudla B, de Herder WW, et al. ENETS Consensus Guidelines for the Standards of Care in Neuroendocrine Tumors: peptide receptor radionuclide therapy with radiolabeled somatostatin analogs. Neuroendocrinology. 2009;90:220-6. doi:10.1159/000225951.
17. Dorr U, Rath U, Sautter-Bihl ML, Guzman G, Bach D, Adrian HJ, et al. Improved visualization of carcinoid liver metastases by indium-111 pentetreotide scintigraphy following treatment with cold somatostatin analogue. Eur J Nucl Med. 1993;20:431-3. doi:10.1007/BF00209003.
18. Ayati N, Lee ST, Zakavi R, Pathmaraj K, Al-Qatawna L, Poon A, et al. Long-Acting Somatostatin Analog Therapy Differentially Alters (68)Ga-DOTATATE Uptake in Normal Tissues Compared with Primary Tumors and Metastatic Lesions. J Nucl Med. 2018;59:223-7. doi:10.2967/jnumed.117.192203.
19. Galne A, Almquist H, Almquist M, Hindorf C, Ohlsson T, Nordenstrom E, et al. A Prospective Observational Study to Evaluate the Effects of Long-Acting Somatostatin Analogs on (68)Ga-DOTATATE Uptake in Patients with Neuroendocrine Tumors. J Nucl Med. 2019;60:1717-23. doi:10.2967/jnumed.119.226332.
20. Hukovic N, Panetta R, Kumar U, Patel YC. Agonist-dependent regulation of cloned human somatostatin receptor types 1-5 (hSSTR1-5): subtype selective internalization or upregulation. Endocrinology. 1996;137:4046-9. doi:10.1210/endo.137.9.8756582.
21. Sabet A, Nagarajah J, Dogan AS, Biersack HJ, Sabet A, Guhlke S, et al. Does PRRT with standard activities of 177Lu-octreotate really achieve relevant somatostatin receptor saturation in target tumor lesions?: insights from intra-therapeutic receptor imaging in patients with metastatic gastroenteropancreatic neuroendocrine tumors. EJNMMI research. 2013;3:82. doi:10.1186/2191-219x-3-82.
22. Aalbersberg EA, de Wit-van der Veen BJ, Versleijen MWJ, Saveur LJ, Valk GD, Tesselaar MET, et al. Influence of lanreotide on uptake of (68)Ga-DOTATATE in patients with neuroendocrine tumours: a prospective intra-patient evaluation. Eur J Nucl Med Mol Imaging. 2019;46:696-703. doi:10.1007/s00259-018-4117-x.
23. Velikyan I, Sundin A, Eriksson B, Lundqvist H, Sorensen J, Bergstrom M, et al. In vivo binding of [68Ga]-DOTATOC to somatostatin receptors in neuroendocrine tumours--impact of peptide mass. Nucl Med Biol. 2010;37:265-75. doi:10.1016/j.nucmedbio.2009.11.008.
24. Lodge MA, Solnes LB, Chaudhry MA, Wahl RL. Prospective Within-Patient Assessment of the Impact of an Unlabeled Octreotide Pre-dose on the Biodistribution and Tumor Uptake of (68)Ga DOTATOC as Assessed by Dynamic Whole-body PET in Patients with Neuroendocrine Tumors: Implications for Diagnosis and Therapy. Mol Imaging Biol. 2021;23:766-74. doi:10.1007/s11307-021-01600-5.
25. Jahn U, Ilan E, Velikyan I, Fross-Baron K, Lubberink M, Sundin A. Receptor depletion and recovery in small-intestinal neuroendocrine tumors and normal tissues after administration of a single intravenous dose of octreotide measured by (68)Ga-DOTATOC PET/CT. EJNMMI Res. 2021;11:118. doi:10.1186/s13550-021-00860-0.

26. Patlak CS, Blasberg RG. Graphical evaluation of blood-to-brain transfer constants from multiple-time uptake data. Generalizations. J Cereb Blood Flow Metab. 1985;5:584-90. doi:10.1038/jcbfm.1985.87.
27. Ilan E, Sandstrom M, Velikyan I, Sundin A, Eriksson B, Lubberink M. Parametric Net Influx Rate Images of (68)Ga-DOTATOC and (68)Ga-DOTATATE: Quantitative Accuracy and Improved Image Contrast. J Nucl Med. 2017;58:744-9. doi:10.2967/jnumed.116.180380.
28. Jahn U, Garske-Román U, Sandström M, Lubberink M, Sundin A. Impact of administered amount of peptide on tumor dosimetry at the first cycle of peptide receptor radionuclide therapy (PRRT) in relation to total tumor somatostatin receptor expression. EJNMMI research. 2023;13:45. doi:10.1186/s13550-023-00997-0.
29. Scoazec JY. Angiogenesis in neuroendocrine tumors: therapeutic applications. Neuroendocrinology. 2013;97:45-56. doi:10.1159/000338371.
30. Jahn U, Ilan E, Sandstrom M, Lubberink M, Garske-Roman U, Sundin A. Peptide Receptor Radionuclide Therapy (PRRT) with (177)Lu-DOTATATE; Differences in Tumor Dosimetry, Vascularity and Lesion Metrics in Pancreatic and Small Intestinal Neuroendocrine Neoplasms. Cancers (Basel). 2021;13. doi:10.3390/cancers13050962.
31. Haug AR, Rominger A, Mustafa M, Auernhammer C, Goke B, Schmidt GP, et al. Treatment with octreotide does not reduce tumor uptake of (68)Ga-DOTATATE as measured by PET/CT in patients with neuroendocrine tumors. J Nucl Med. 2011;52:1679-83. doi:10.2967/jnumed.111.089276.
32. Reubi JC, Horisberger U, Studer UE, Waser B, Laissue JA. Human kidney as target for somatostatin: high affinity receptors in tubules and vasa recta. J Clin Endocrinol Metab. 1993;77:1323-8. doi:10.1210/jcem.77.5.7915721.
33. Balster DA, O'Dorisio MS, Summers MA, Turman MA. Segmental expression of somatostatin receptor subtypes sst(1) and sst(2) in tubules and glomeruli of human kidney. Am J Physiol Renal Physiol. 2001;280:F457-65. doi:10.1152/ajprenal.2001.280.3.F457.
34. Kamaldeep, Loharkar S, Das T, Basu S, Banerjee S. Estimation of Absorbed Doses of Indigenously Produced "Direct-route" Lutetium-177-[(177)Lu]Lu-DOTA-TATE PRRT in Normal Organs and Tumor Lesions in Patients of Metastatic Neuroendocrine Tumors: Comparison with No-Carrier-Added [(177)Lu]Lu-DOTA-TATE and the Trend with Multiple Cycles. Cancer Biother Radiopharm. 2022;37:214-25. doi:10.1089/cbr.2021.0340.
35. Forrer F, Krenning EP, Kooij PP, Bernard BF, Konijnenberg M, Bakker WH, et al. Bone marrow dosimetry in peptide receptor radionuclide therapy with [177Lu-DOTA(0),Tyr(3)]octreotate. Eur J Nucl Med Mol Imaging. 2009;36:1138-46. doi:10.1007/s00259-009-1072-6.